Biological cell submitted to a ns electrical pulse

Noël Burais, François Buret, Nicolas Faure, Laurent Nicolas, Ronan Perrussel

Biological cell submitted to a ns electrical pulse

Noël Burais, François Buret, Nicolas Faure, Laurent Nicolas and Ronan Perrussel
Laboratoire Ampère (UMR CNRS 5005), Université de Lyon, Lyon, France
nicolas.faure@ec-lyon.fr, ronan.perrussel@ec-lyon.fr

***Abstract*—This work tackles the development of numerical methods in order to study the influence of a nanosecond electrical pulse on the phenomena arising in a biological cell. Formulations employed are presented and applied to the observation of the sensitivity of an eukaryote cell to the orientation of the electric field.**

***Index Terms*—Bioelectric field computation, asymptotic model, axisymmetric formulation.**

I. Introduction

Biological assemblies are sensitive to electrical perturbations. Thus, high voltage microsecond (ms) pulses can interact with living organisms, allowing for example modifications of the cytoplasmic membrane structures in biological cells. One of these modifications is called *electropermeabilization* or *electroporation* [1]. This phenomenon is related to the *transmembrane potential* (TMP) that is defined as the potential difference between the outside and inside faces of a membrane.

New applied developments are running in the fields of Biotechnology and clinical drug delivery. The safe use of these approaches requires a deep knowledge of the involved space and time-dependent mechanisms. Both molecular dynamics and preliminary experimental approaches indicate that the *key steps are present on the nanosecond (ns) time scale*. Recently, it was found that electromagnetic pulses of even shorter duration (order of 10 nanoseconds) can also modify the membranes of biological cell constituents such as the nucleus or the mitochondria without noticeably altering the cell membrane [2], [3]. Results from the literature show that *cancerous tumors* can be reduced in size by applying a limited number of voltage pulses with very fast rise time [4]. The published works also demonstrate very promising potential applications of these ultra short high voltage pulses for *gene transfer*.

In this work, the objective is the development of the basic numerical tools in order to compute the different phenomena arising in the cell when exposed to a ns electrical pulse and to understand the influence of the main physical and electrical parameters on these phenomena. First, the models and methods used are recalled. Then, some results on an eukaryote cell are presented for a pulse of 10 ns duration. In particular, the influence of the cell orientation with regard to the electric field is quantified.

II. Models and methods

The cell model is composed by a *conductive cytoplasm* and a *conductive nucleus*, each being surrounded by an *insulating membrane*. As this stage, some complex materials locate inside the cell, as mitochondria or endoplasmic reticulum, are not modelled. The geometrical and electrical parameters of the cell considered in this work — coming from the relevant literature [5] — are given in Fig. 1. The exposure system consists of two parallel and plane electrodes between which a conductive medium, containing the cell, is placed. Indeed, the aim is to obtain an homogeneous electric field in which the cell is immersed.

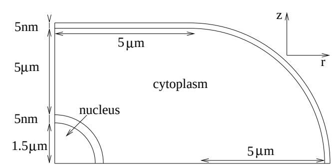

region	σ(S/m)	ϵ_r
nucl. cyto.	0.3	80
nucl. memb.	10^{-9}	5
cell cyto.	0.3	80
cell memb.	10^{-9}	5
exterior bath	1.2	80

Fig. 1. $1/4$ of the geometry of the cell considered in this work (z-axis is an axis of revolution) and its electrical parameters. cyto., memb. and nucl. are respectively for cytoplasm, membrane and nucleus.

Our approach is based on the *electro-quasistatic formulation* in the time-transient case:

$$\begin{cases} -\operatorname{div}\left(\left(\varepsilon\dfrac{\partial}{\partial t}+\sigma\right)\operatorname{grad}(V)\right)=0, \\ V=V_{\mathrm{imp}}(t) \text{ or } \dfrac{\partial V}{\partial \mathbf{n}}=0 \text{ on the boundary,} \end{cases} \tag{1}$$

or in the time-harmonic case:

$$\begin{cases} -\operatorname{div}\left((i\omega\varepsilon+\sigma)\operatorname{grad}(V)\right)=0 \\ + \text{ same type of boundary conditions.} \end{cases} \tag{2}$$

Here σ and ϵ denote respectively the conductivity and the permittivity of the medium, V the electric potential (V_{imp} is enforced on the electrodes) and $\mathbf{n}$ is the unitary outgoing normal of the domain. For the time-harmonic case, ω is the angular frequency. It is discretized by using the *finite element method* and the implementation is based on the getfem++ finite element library [6]. P_2-Lagrange finite element are considered for the spatial discretization and a Crank-Nicholson scheme is used for the time discretization when necessary.

A. Transmission conditions

In order to avoid meshing the thin membranes — consider 5 nm of thickness compared to 1.5 μm for the radius of the nucleus — an *interface* Σ *is used to replace the membrane* and *approximate transmission conditions* are enforced on Σ

[7], [8]. The full transmission conditions for a 3D and time-transient problem should be:

$$\begin{cases} \left(\varepsilon_m \dfrac{\partial}{\partial t} + \sigma_m\right) [V]_\Sigma \\ = \delta \left(\left(\varepsilon_e \dfrac{\partial}{\partial t} + \sigma_e\right) - \left(\varepsilon_m \dfrac{\partial}{\partial t} + \sigma_m\right) \right) \left(\dfrac{\partial V}{\partial \mathbf{n}}\right)_{|\Sigma_e}, \\ \left[\left(\varepsilon \dfrac{\partial}{\partial t} + \sigma\right) \dfrac{\partial V}{\partial \mathbf{n}}\right]_\Sigma \\ = \delta \left(\left(\varepsilon_e \dfrac{\partial}{\partial t} + \sigma_e\right) - \left(\epsilon_m \dfrac{\partial}{\partial t} + \sigma_m\right) \right) \triangle_\Sigma (V_{|\Sigma_e}). \end{cases} \tag{3}$$

In conditions (3), δ is the thickness of the membrane and $[\cdot]_\Sigma$ denotes a jump of the quantity on Σ — for instance $[V]_\Sigma = V_{|\Sigma_e} - V_{|\Sigma_i}$ where $\cdot_{|\Sigma_e}$ (resp. $\cdot_{|\Sigma_i}$) refers to the restriction to Σ on the exterior side (resp. interior side). The indexes i, e and m indicate respectively interior medium, exterior medium and membrane properties and $\triangle_\Sigma$ is the Laplace-Beltrami operator on the interface Σ.

Because of the value of the membrane parameters — indeed for each membrane σ_m and ε_m are small compared to $\sigma_i,\ \sigma_e$ and $\varepsilon_i,\ \varepsilon_e$— we more simply assume that:

$$\begin{cases} \left(\varepsilon_m \dfrac{\partial}{\partial t} + \sigma_m\right) [V]_\Sigma = \delta \left(\varepsilon_e \dfrac{\partial}{\partial t} + \sigma_e\right) \left(\dfrac{\partial V}{\partial \mathbf{n}}\right)_{|\Sigma_e}, \\ \left[\left(\varepsilon \dfrac{\partial}{\partial t} + \sigma\right) \dfrac{\partial V}{\partial \mathbf{n}}\right]_\Sigma = 0. \end{cases} \tag{4}$$

It can be recognized as a contact resistance model. In the context of this work, it seems *sufficiently accurate for the computation of the TMP*. This accuracy is assessed by Fig. 2 for the time-transient case. In this test, the cell of Fig. 1 is submitted to a ns pulse; the TMP is computed at the location where it is maximal on the membrane and the results obtained, considering a model with and without the transmission conditions, are compared. The relative error is overall strictly less than 3% for the cell (Fig. 2(a)) and the nucleus (Fig. 2(b)).

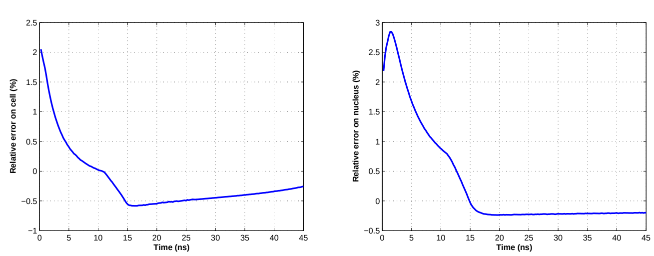

(a) TMP on the cell. (b) TMP on the nucleus.

Fig. 2. Relative error between models with or without the transmission conditions in the time-transient case. Pulse is the same as in Fig. 9(a). Membranes are supposed to be 10 nm thick in order to simplify the mesh for the computations without the transmission conditions.

Is is also performed a test of the accuracy in the range of frequency which is of interest here. Fig. 3 shows roughly two states for the relative error obtained: at low frequency, the accuracy is mainly related to the ratio σ_m/σ_e which is close to zero and consequently the error is small and at high frequency, the accuracy is related to the ratio $\varepsilon_m/\varepsilon_e$ which is less favorable (but still small compared to one) and consequently the error increases (but stays reasonable).

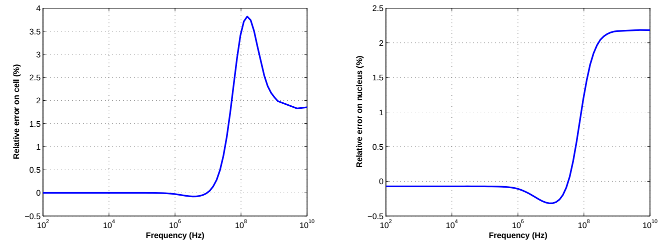

(a) TMP on the nucleus. (b) TMP on the cell.

Fig. 3. Relative error between models with or without transmission conditions in the time-harmonic case vs the frequency.

B. *Complements on the axisymmetric formulation*

For the 3D-axisymmetric problem it is considered a source electric field — linked to the location of the electrodes — *whose relative orientation with the cell is not necessarily following the cell axis of revolution*. As the problem considered is linear, the source electric field is decomposed on its component following this axis of revolution $\mathbf{E}_\mathrm{z}$ and its component in the orthogonal of this axis $\mathbf{E}_\mathrm{r}$. The plane defined by the directions of $\mathbf{E}_\mathrm{z}$ and $\mathbf{E}_\mathrm{r}$ and containing the origin is the plane where all the computations can be done. Two problems are required to be solved:

- the first problem with solution V_z uses the classical boundary conditions on Fig. 4(a) and the sesquilinear form (expressed in the time-harmonic case here):

$$\int_\Omega (i\omega\varepsilon + \sigma)\, r \left(\frac{\partial V_\mathrm{z}}{\partial r}\frac{\partial v}{\partial r} + \frac{\partial V_\mathrm{z}}{\partial z}\frac{\partial v}{\partial z}\right) drdz + \sum_{k=1}^{2} \int_{\Sigma_k} \frac{(\mathrm{i}\omega\varepsilon_{m_k} + \sigma_{m_k})}{\delta_k} r [V_\mathrm{a}]_{\Sigma_k} [v]_{\Sigma_k} ds. \tag{5}$$

- the second problem with a solution V_r uses the boundary conditions on Fig. 4(b) and the sesquilinear form:

$$\int_\Omega (\mathrm{i}\omega\varepsilon + \sigma)\, r \left(\frac{\partial V_\mathrm{r}}{\partial r}\frac{\partial v}{\partial r} + \frac{\partial V_\mathrm{r}}{\partial z}\frac{\partial v}{\partial z}\right) drdz + \int_\Omega \frac{(\mathrm{i}\omega\varepsilon + \sigma)}{r} V_\mathrm{r} v drdz + \sum_{k=1}^{2} \int_{\Sigma_k} \frac{(\mathrm{i}\omega\varepsilon_{m_k} + \sigma_{m_k})}{\delta_k} r [V_\mathrm{r}]_{\Sigma_k} [v]_{\Sigma_k} ds \tag{6}$$

The electric potential in the whole space is finally obtained using both solution: $V(r,z,\theta) = V_\mathrm{z}(r,z) + V_\mathrm{r}(r,z)\cos(\theta)$ where θ is the angular coordinate around the axis of revolution. This decomposition has been validated on a sphere geometry with several possibilities for the orientation of the field.

III. Time-harmonic results

A frequency response of the cell is shown in the top of Fig. 5 when submitted to an electric field following the axis of revolution. The dashed lines describe the behavior of the

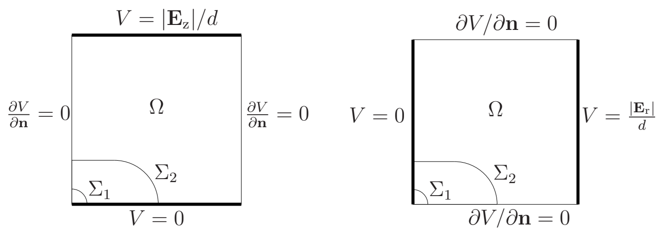

(a) $\mathbf{E}_z$. (b) $\mathbf{E}_r$.

Fig. 4. Boundary conditions for the two components of the electric field. Distance d is the side length of the domain.

TMPs of the nucleus and of the cell, the solid line is the ratio between both TMPs. Until 100 kHz the nucleus is shielded by the membrane of the cell. Between 100 kHz and 2 MHz the electric field penetrates into the cytoplasm and the TMP of the nucleus increases. After 100 MHz, the entire cell is transparent to the field. The bottom of Fig. 5 shows the spectrum of pulses of respectively 10 ns and 10 ms duration: by superimposing the top and bottom figures, it appears that only the ns pulse contains the frequency components to influence the nucleus.

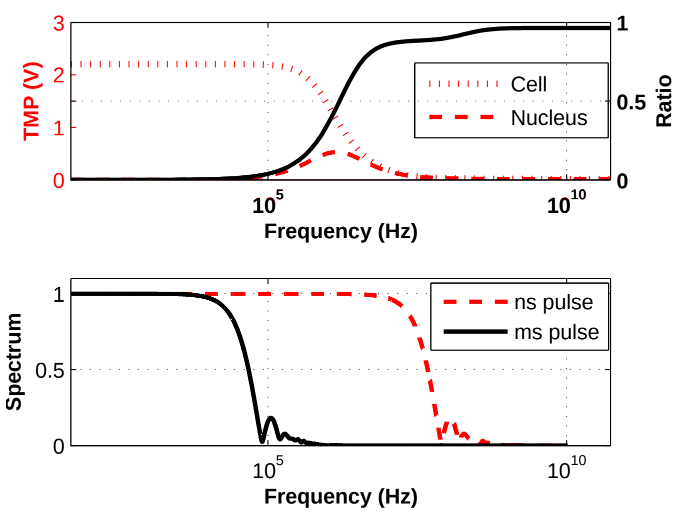

Fig. 5. Time-harmonic response of the cell and normalized spectrum of ns and ms pulses. Source $\mathbf{E}$-field: $2 \cdot 10^5$ V/m, along z-axis.

Fig. 6 shows the scalar potential cartography and the associated electric field lines for four frequencies: 10 kHz, 1 MHz, 3 MHz and 1 GHz. For frequencies until 10 kHz there is a zero electric field inside the cell. In this case it is impossible to reach the nucleus because of the *shielding effect* of the cell membrane. Around 2 MHz, there is a penetration of the field inside the cytoplasm of the cell and there is a zero field inside the nucleus. This configuration could be the most adapted to obtain the electropermeabilization of the nucleus membrane. For higher frequencies the field penetrates in the entire cell. These results show the sensitivity of the nucleus to a ns pulse and the feasibility of the permeabilization of the membrane of the nucleus with an adapted pulse amplitude.

Fig. 7 shows the sensitivity of the TMPs to the relative orientation of the source electric field with the cell at several frequencies; let ϕ be the parameter quantifying this relative orientation, $\phi = 0^\bullet$ corresponds to the case $\mathbf{E}_r = 0$ (see Fig. 4(a)) and consequently $\phi = 90^\bullet$ will correspond to the case $\mathbf{E}_z = 0$ (see Fig. 4(b)). The value of the TMP on the membrane of the cell is the highest if the electrodes are perpendicular to the smallest axis of the cell, *i.e.* $\phi = 0^\bullet$, while the TMP of the nucleus is the highest if the electrodes are perpendicular to the longest axis of the cell, *i.e.* $\phi = 90^\bullet$. This conclusion is valid only for frequencies lower than 10 MHz.

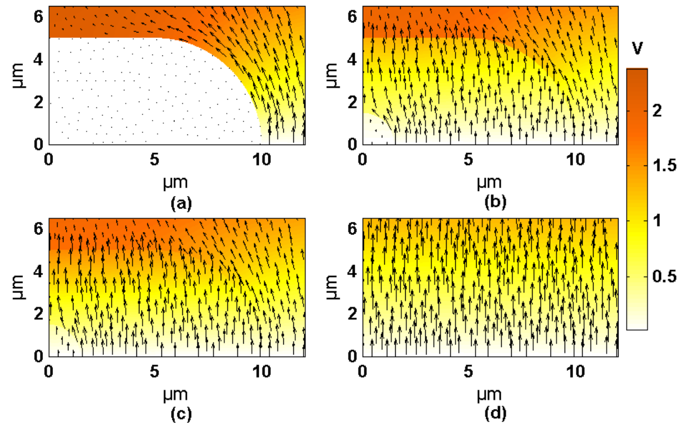

Fig. 6. Time-harmonic cartography of scalar potential with electric field lines at (a) 10 kHz, (b) 1 MHz, (c) 3 MHz, (d) 1 GHz. Source $\mathbf{E}$-field along z-axis.

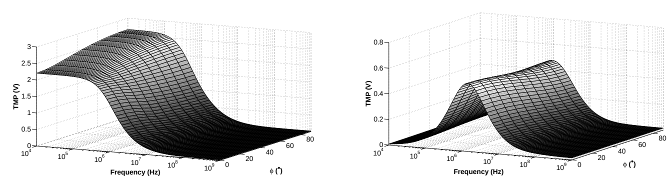

(a) TMP on the cell. (b) TMP on the nucleus.

Fig. 7. Maximal TMP on the membrane vs the orientation of the $\mathbf{E}$-field and the frequency.

IV. Time-Transient Simulation

The cell of Fig. 1 is exposed to a pulse of 10 ns duration, of 1 ns rise time, of 4 ns fall time. Different values for the parameter ϕ were tested. Fig. 8 sums up the results obtained by showing the decrease of the TMP of the cell and of the nucleus by going from $\phi = 0^\bullet$ to $\phi = 90^\bullet$. The results of the two extreme configurations, recalled Fig. 4(a) and 4(b), are shown Fig. 9(a) and Fig. 9(b).

For each exposure configuration, The TMP of the cell is upper than the TMP of the nucleus. This result agree with time-harmonic results shown Fig. 7 where the ratio between the TMPs of the cell and the nucleus is less than 1, in the frequency range. The most important result is the difference in the TMP between the configuration $\phi = 90^\bullet$ and the configuration $\phi = 0^\bullet$. In the case of the cell, the increase

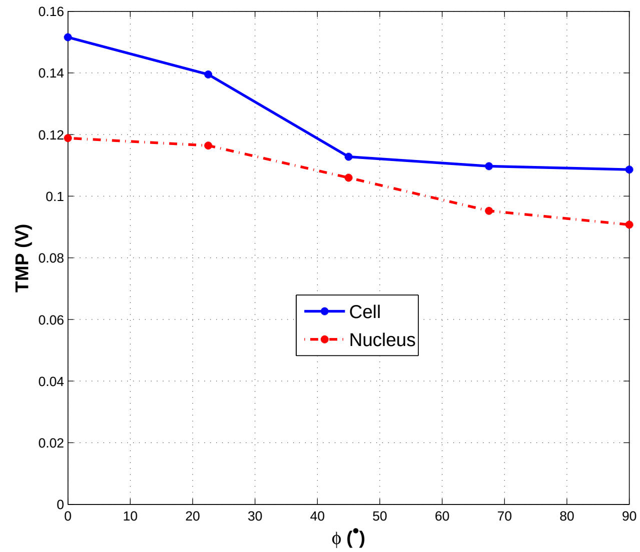

Fig. 8. Maximal TMP on the membrane vs the orientation of the **E**-field.

of the TMP is around 40% while in the case of nucleus it is around 30%.

The results can explain why for a fixed amplitude of the pulse, some cells should be electroporated while others are not, depending of the orientation of each cell. This type of study may predict the amplitude and the duration of the pulse to activate the permeabilization phenomena in the membrane of the nucleus; after the activation, a more precise description of this non-linear phenomena have to be done.

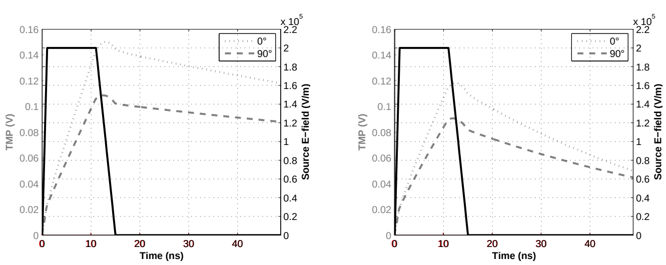

(a) TMP on the cell. (b) TMP on the nucleus.

Fig. 9. Time-transient response of the membranes to a ns pulse.

V. Conclusion

It is presented in this work basic numerical tools for dealing with a cell submitted to ns pulse, with a particular emphasis on the membrane and a proper model of 3D-axisymmetric phenomenon. It enables to simply interpret how some type of ns pulse can act directly on the membrane of the nucleus and also that non purely spherical shape cell can react differently depending of their orientation relatively to the electric field. Our objective is also to incorporate non-linear electroporation effects for further study of the phenomenon as it has already proposed in [9], [10] for plane 2D phenomena; it should lead to full 3D computations.

Acknowledgment

The authors thank Clair Poignard for many fertile discussions. The financial support of the Agence Nationale de la Recherche concerning the project Cemirbio is also gratefully acknowledged.

References

[1] B. Gabriel and J. Teissié, "Time courses of mammalian cell electropermeabilization observed by millisecond imaging of membrane property changes during the pulse," *Biophys. J.*, vol. 76, pp. 2158–2165, 1999.

[2] S. J. Beebe, "Nanosecond pulsed electric fields: A new stimulus to activate intracellular signaling," *Journal of Biomedicine and Biotechnology*, vol. 2005, pp. 297–300, 2005.

[3] W. Frey, J. A. White, R. O. Price, P. F. Blackmore, R. P. Joshi, R. Nuccitelli, S. J. Beebe, K. H. Schoenbach, and J. F. Kolb, "Plasma membrane voltage changes during nanosecond pulsed electric field exposure," *Biophysical Journal*, vol. 90, pp. 3608–3615, 2006.

[4] N. Chen, K. H. Schoenbach, J. F. Kolb, R. J. Swanson, A. L. Garner, J. Yang, R. P. Joshi, and S. J. Beebe, "Leukemic cell intracellular responses to nanosecond electric fields," *Biochemical and Biophysical Research Communications*, vol. 317, pp. 421–427, 2004.

[5] T. Kotnik and D. Miklavčič, "Theoretical evaluation of voltage inducement on internal membranes of biological cells exposed to electric fields." *Biophys. J.*, vol. 90, no. 2, pp. 480–491, Jan 2006.

[6] Y. Renard and J. Pommier, Getfem finite element library. http://home.gna.org/getfem/.

[7] C. Poignard, "Asymptotics for steady state voltage potentials in a bidimensionnal highly contrasted medium with thin layer," *Math. Meth. Appl. Sci.*, vol. 31, no. 4, pp. 443 – 479, July 2007, doi: 10.1002/mma.923.

[8] C. Poignard, P. Dular, R. Perrussel, L. Nicolas, L. Krähenb"uhl, and M. Schatzman, "Approximate conditions replacing thin layers," To appear in IEEE Trans. on Mag., preprint available at the url https://hal.archives-ouvertes.fr/hal-00165049.

[9] D. A. Stewart, T. R. Gowrishankar, and J. C. Weaver, "Transport lattice approach to describing cell electroporation: use of a local asymptotic model," *Plasma Science, IEEE Transactions on*, vol. 32, pp. 1696–1708, Aug. 2004. [Online]. Available: http://epore.mit.edu/abstracts/2004_1.html

[10] K. Smith, T. Gowrishankar, A. Esser, D. Stewart, and J. Weaver, "The spatially distributed dynamic transmembrane voltage of cells and organelles due to 10 ns pulses: Meshed transport networks," *Plasma Science, IEEE Transactions on*, vol. 34, no. 4, pp. 1394–1404, Aug. 2006.